## ONLINE SUPPLEMENT

### Supplemental Methods

### Luxol fast blue (LFB) staining

LFB staining was used to detect any histological changes in white matter. In brief, brain slices were incubated with 0.1% LFB (G1030, Goodbio technology CO. LTD, Wuhan, China) at 60 ℃ overnight and imaged by light microscopy (DP 50, Olympus, Japan). The white matter lesions were evaluated in five regions: the optic tract, internal capsule, fiber bundles within the striatum, corpus callosum, and anterior commissure. Mann–Whitney U test was used to compare the severity of WM lesions between the groups.

### 5-bromo-4-chloro-3-indolyl-β-d-galactopyranoside (X-gal) staining

For detection of Cre-recombinase expression and biocytin visualization, brains were removed after transcardial perfusion, post-fixed in 4% PFA for 2 h (4 ℃), cryoprotected using 30% sucrose in PBS, and cut in the coronal plane as 30-μm-thick slices, which were then processed for ß-galactosidase expression using X-gal staining, as described elsewhere [1, 2]. In brief, brain tissues were transferred to 5-bromo-4-chloro-3-indolyl-beta-D-galactopyranoside (X-gal) solution (1 mg/ml X-gal, 5 mM potassium ferricyanide, 5 mM potassium ferrocyanide, 2 mM $MgCl_2$, 0.01% sodium deoxycholate, and 0.02% Nonidet P-40, in PBS) in multi-well plates, and then incubated at 37 ℃ with gentle agitation until clearly-defined staining was achieved.

Free-floating slices were next processed with DAB biocytin detection, and incubated with anti-GFAP antibodies followed by biotin-tagged secondary antibody and Vectasta in Elite ABC reagent (Vector Laboratories, Inc. Burlingame, CA, USA) for 24 h. The DAB reaction proceeded for five minutes. After that, the slices were transferred to microslides and imaged by light microscopy (Olympus, Japan).

### Western blots analysis

Western blots were performed to investigate changes in the expression of MAG, MBP,

NF and β-actin. Mouse brains were rapidly excised and fast frozen in chilled isopentane, and the white matter tissue dissected for protein extraction as described [3] with modification. WM tissue, including corpus callosum, anterior commissure, the internal capsule, optic tract and fimbria of hippocampus, have all been dissected. WM protein was then homogenized in 4 °C with RIPA buffer solution for protein extraction. The protein concentration was determined by the Bradford method using bovine serum albumin (BSA) as the standard. A portion (40 ug) of each sample extract was then resolved on 12% sodium dodecyl sulfate–polyacrylamide gel electrophoresis (SDS–PAGE), blotted, and incubated overnight with the primary antibodies, including anti-β-actin (1:5000, Boster, China), anti-MAG (1:200), anti-MBP (1:500), and anti-Neurofilament-L, M, and H (1:1000) at 4 °C. The membranes were then incubated for one hour at room temperature with horseradish peroxidase-labeled anti-mouse, anti-goat or anti-rat secondary antibody (1:5000, Boster, China). The membranes were visualized with enhanced chemiluminescence kits (Thermo Fisher Scientific, Pierce, USA), and the intensity of blots was semi-quantified using ImageJ (NIH, USA).

**Electron microscopy**

Tissue samples were prepared and tested by electronic microscopy (EM) as previously described [4]. In brief, mice were anesthetized deeply and perfused intracardially with and 2.5% glutaraldehyde in 4% PFA. Brains were removed and coronal sections (1 mm thick) containing corpus callosum were cut on a vibratome, and then post-fixed in osmium tetroxide, dehydrated through graded concentrations of ethanol, pre-embedded with propylene oxide, and flat-embedded in epoxy resin. Samples were processed for routine EM observation and examined in an electron microscope (Hitachi, HT7700) at 120 kV.

At 1000× magnification, the ratio of myelin sheath thickness to axon diameter (g ratio) was calculated for 200 fibers in the corpus callosum from mouse groups using ImageJ. The g ratio was plotted against the diameter of axons to directly compare the extent of myelination around axons of a given size.

**Eight-arm radial maze test**

Spatial learning and working memory were examined using an eight-arm radial maze test, according to previously described methods [5]. The eight-arm radial maze test was started at one month post-surgery, and was conducted consecutively over seven training days followed by nine test days. Animals were deprived of food 12 hours per day for one week prior to testing and pretrained to consume for a 5-min period (one session per mouse) food pellets scattered over the whole maze, extending from the center to the distal end of each arm.

Maze acquisition trials were performed after these pretraining trials. All eight arms were baited with food pellets and mice were placed on the central platform to freely explore the maze for 15 min. A trial was terminated immediately after all eight pellets were consumed or after 15 min had elapsed. An 'arm visit' was defined as an excursion of at least five cm from the central platform. The number of correct choices made before the first error was recorded, with an error defined as a re-entry into a previously visited arm. In the reference memory task, one of the eight arms was consistently baited by one pellet in a food well, and the trial was terminated immediately after it had been consumed. All behavioral testing and the analysis were performed by blinded investigators.

**Supplemental Figures and Figure Legends**

**Supplementary Fig 1**

**The breeding strategy and identification of astroglial-specific connexin43 conditional knockout mice.**
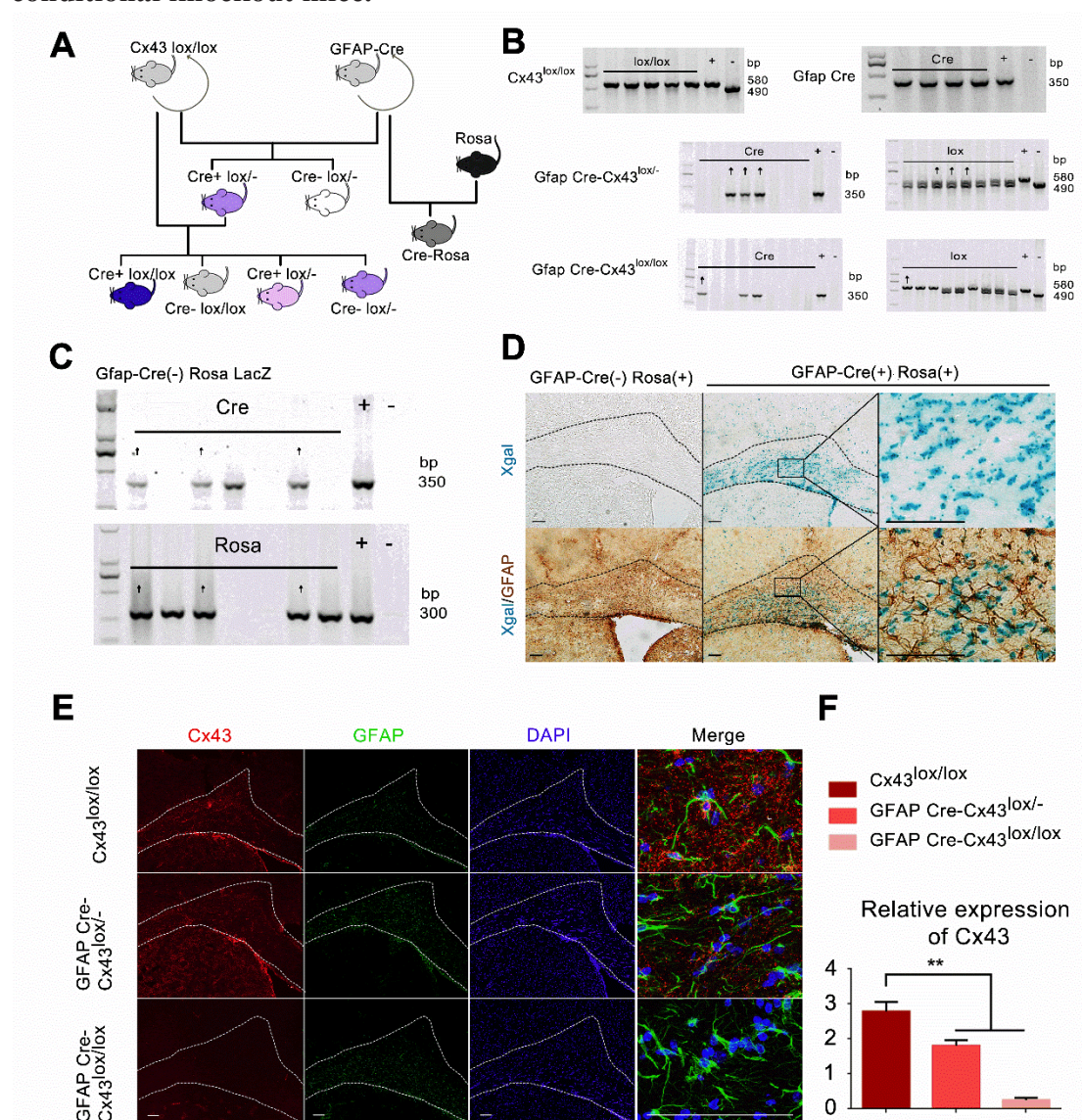


**(A)** Schematic of the breeding strategy for GFAP-Cre$^+$ Cx43$^{fl/fl}$ (Cx43$^{-/-}$) transgenic mice. **(B)** PCR identified four genotypes: Cx43$^{fl/fl}$ genotype, Cx43$^{fl/-}$ genotype, GFAP-Cre$^+$ Cx43$^{fl/-}$ genotype, and GFAP-Cre$^+$ Cx43$^{fl/fl}$ (Cx43$^{-/-}$) genotype. **(C)** PCR identified the GFAP-Cre$^+$ Rosa-LacZ gene. **(D)** X-gal staining of tissues from GFAP-Cre Rosa-LacZ transgenic mice. Scale bar, 100 μm. **(E)** Representative confocal images of coronal sections from Cx43$^{fl/fl}$, GFAP-Cre$^+$ Cx43$^{fl/-}$ (Cx43$^{fl/-}$) and GFAP-Cre$^+$ Cx43$^{fl/fl}$ (Cx43$^{-/-}$) transgenic mice triple-labeled with Cx43/DAPI/GFAP. Scale bar, 100 μm. **(F)** Quantitative analysis of Cx43 expression in **(E)** and the unit for y-axis was $10^3/mm^2$, **$p<0.01$ versus Cx43$^{fl/fl}$, one-way ANOVA with Dunnett's post-hoc test, n=6 mice per group.

**Supplementary Figure 2**
**The flowchart of the experimental design**
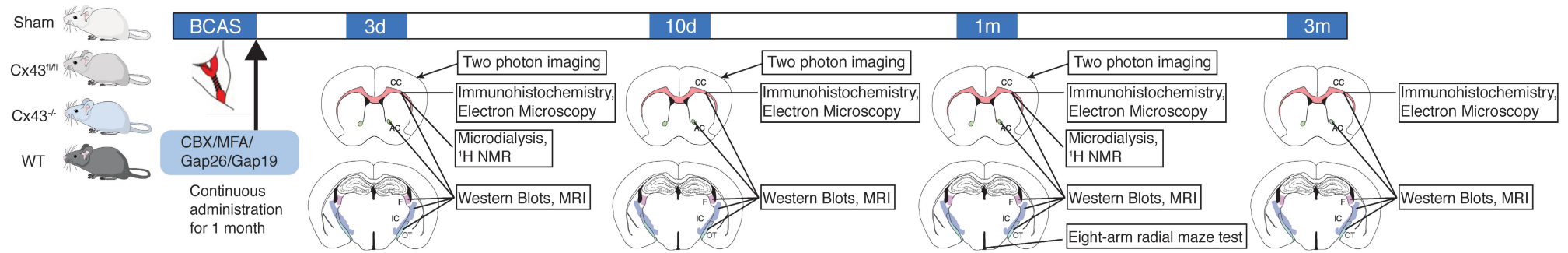


A flowchart of the experiment design depicts the experiments performed at each time point (three days, ten days, one month, and three months) after bilateral carotid common artery stenosis (BCAS) and in sham control mice. (CBX: Carbenoxolone; MFA: Meclofenamic; CC: corpus callosum; AC: anterior commissure; F: fimbria of the hippocampus; IC: internal capsule; OT: optic tract; WT: wide-type)

**Supplementary Figure 3**
**MRI DTI for detection of structural disruption of myelinated axons in BCAS mice.**
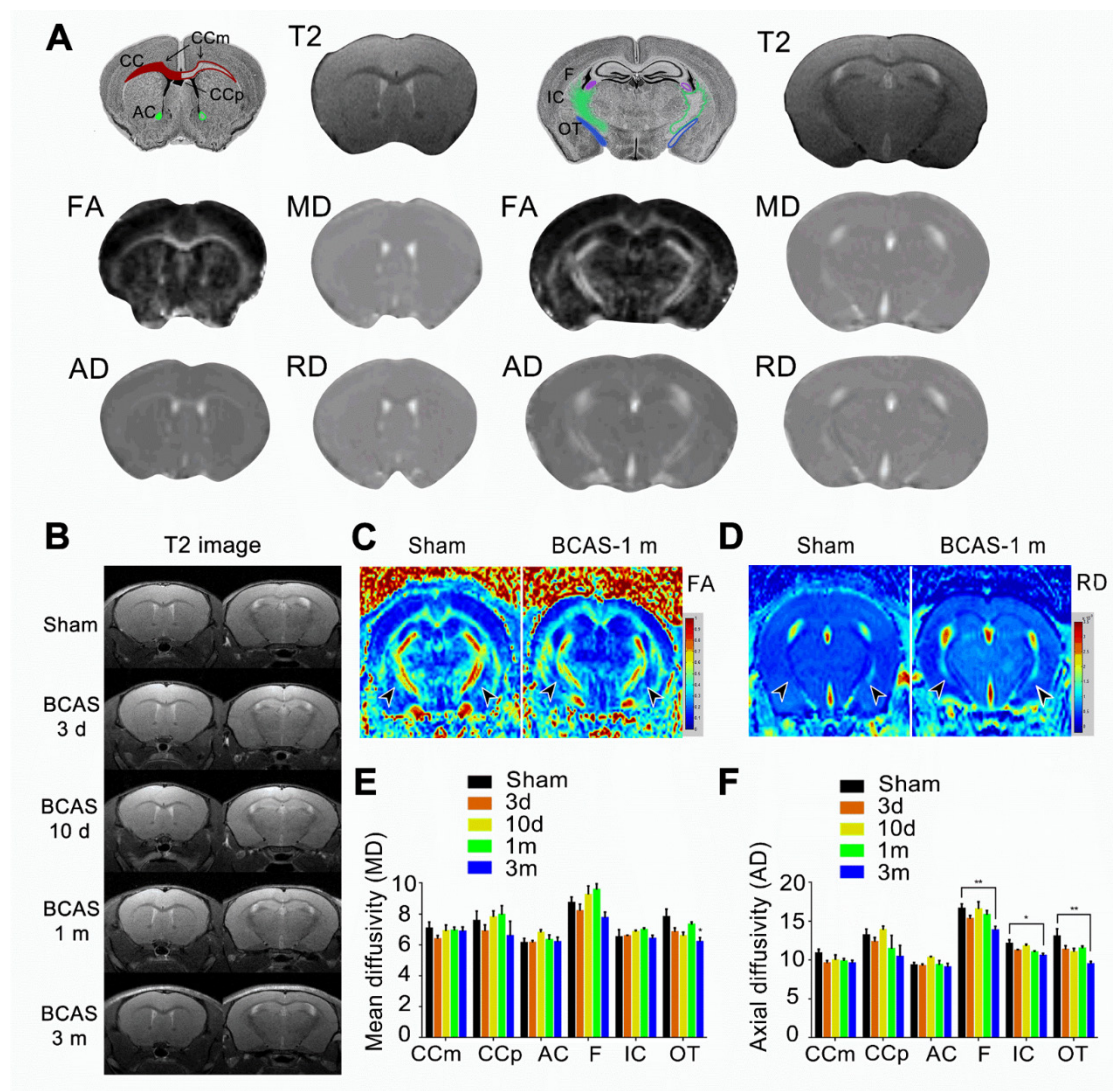


(A) Schematic diagram of 7 T MRI scanning and the selected regions of interest for analysis, which include the medium part of corpus callosum (CCm), peripheral part of corpus callosum (CCp), anterior commissure (AC), fimbria of the hippocampus (F), internal capsule (IC), and optic tract (OT). (B) Representative images of T2 scanning at three days, ten days, one month and three months post-BCAS. (C-D) Representative 7 T MRI images depict the integrity of the myelin sheath and axonal structures in the F, IC, and OT at one month post-BCAS. (E-F) Quantitative analysis of mean diffusivity (MD) and axial diffusivity (AD) values in (B). *$p<0.05$, **$p<0.01$ versus Sham, one-way ANOVA with Dunnett's post-hoc test, n=6 mice for sham and three months, n=5 for three and ten days, and n=7 for one month.

**Supplementary Figure 4**
**Cortical and hippocampal structure was maintained after hypoperfusion injury**
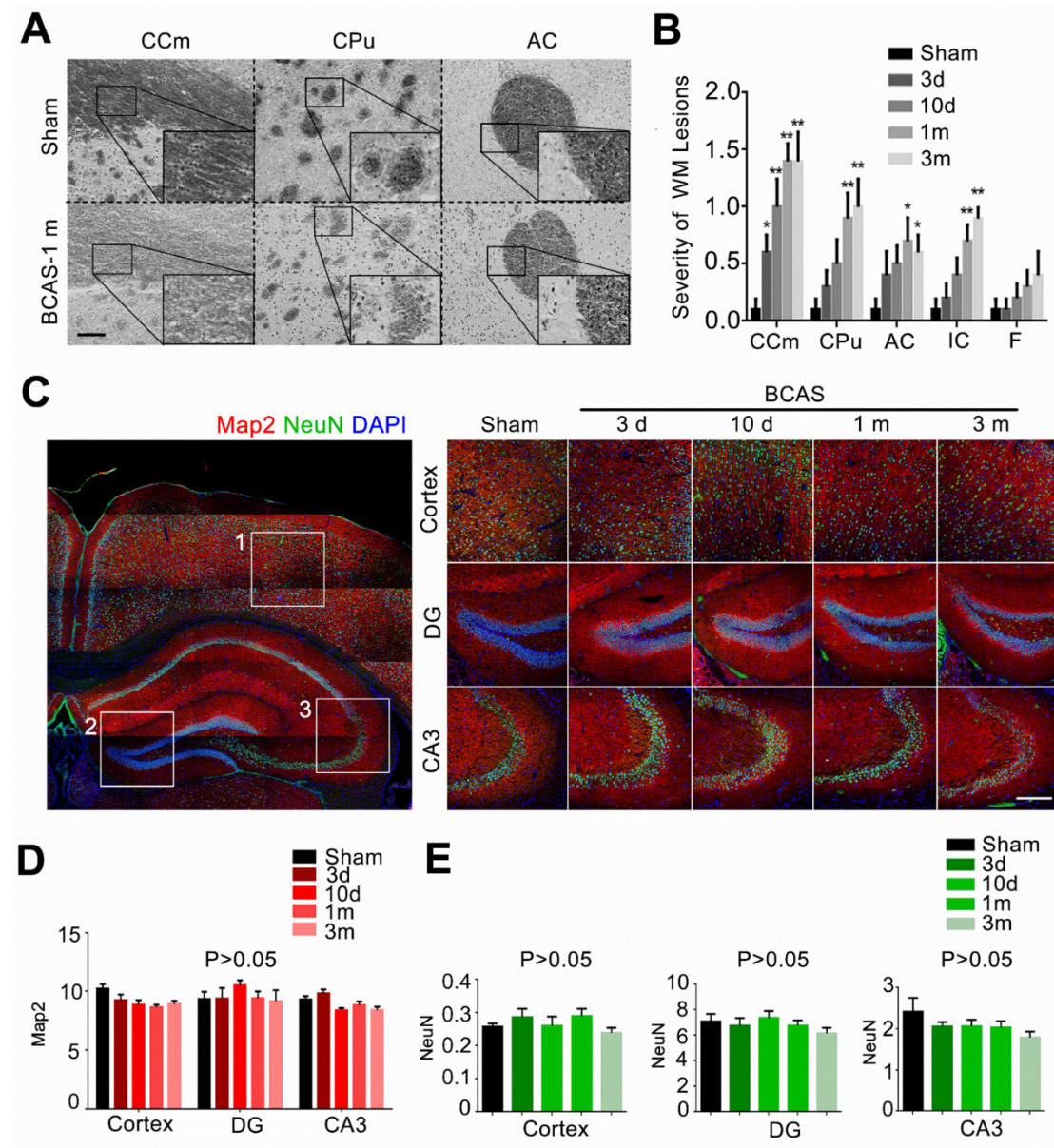


(A) Myelin loss was detected by LFB staining in the medial part of the corpus callosum (CCm), caudate-putamen (CP), anterior commissure (AC), the internal capsule (IC), and fimbria (F) of hippocampus at three days, ten days, one month and three months post-BCAS. Tissue damage was graded 0 to 3, with the most severe rarefaction in the CCm (left). Scale bar, 100 μm. (B) The histogram summarizes the severity of white matter lesions in the medial part of the CCm, CPu, AC, IC, and F at three days, ten days, one month, and three months post-BCAS (right). **p<0.01, *p<0.05 versus Sham, one-way ANOVA with Dunnett's post-hoc test, n=10 mice for each group. (C) Representative confocal images of coronal sections depicting the morphology of cerebral cortex and hippocampus triple-labeled with microtubule-associated protein2 (Map2), neuronal nuclei (NeuN) and 4',6-diamidino-2-phenylindole (DAPI). The white square insets represented the

cerebral cortex, dentate gyrus, and CA3 region in hippocampus. Higher magnification images of the insets in **(C)** demonstrate that there was no morphological disruption at three days, ten days, one month, and three months post-hypoperfusion injury in BCAS mice. Scale bar, 200μm. **(D)** Quantitative analysis of Map2 expression and the unit for y-axis was $10^4/mm^2$, p>0.05 versus Sham, one-way ANOVA with Dunnett's post-hoc test, n=5 mice per group. **(E)** Quantitative analysis of NeuN positive neuron numbers in cerebral cortex, dentate gyrus, and CA3 region in hippocampus at three days, ten days, one month, and three months post-BCAS. The unit for the y-axis was $10^3/mm^2$. p>0.05 versus Sham, one-way ANOVA with Dunnett's post-hoc test, n=4 mice per group.

**Supplementary Figure 5**

**Schematic diagram illustrating the temporal progression of myelin injury and the sensitivity of the alternative approaches for its detection.**
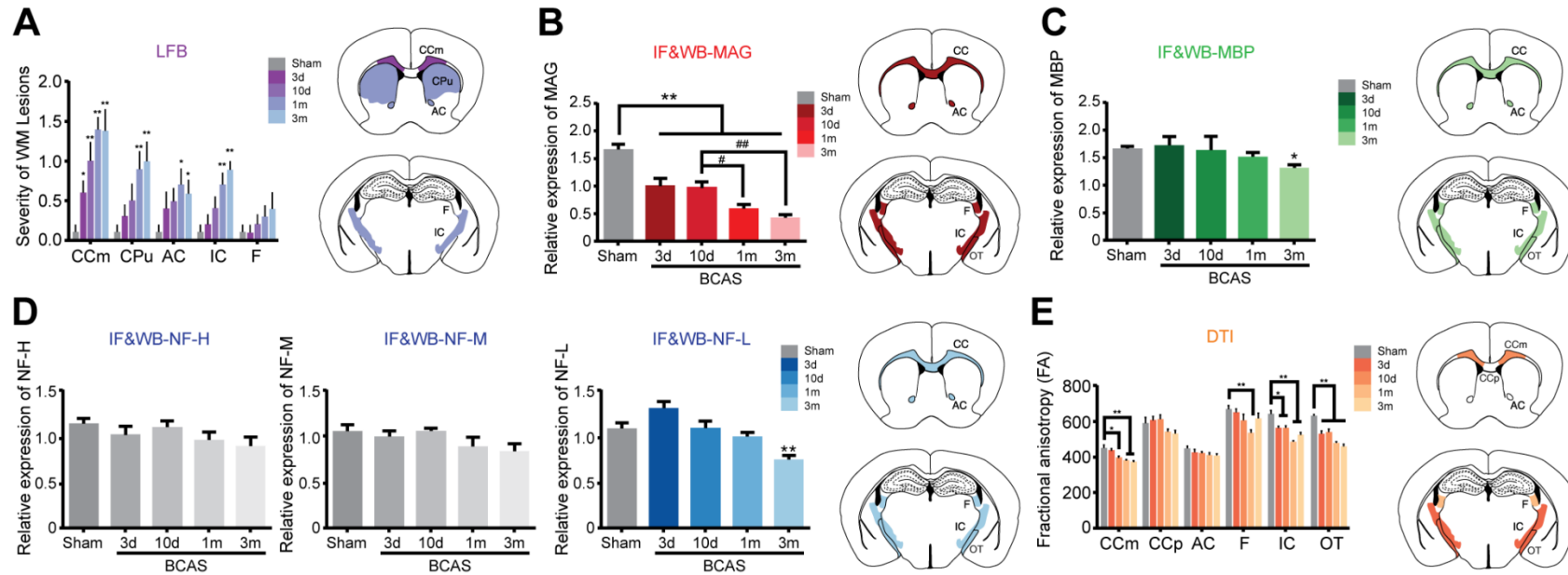


(A) Representative coronal sections illustrate the temporal progression of myelin injury detected by LFB staining, **(B)** by MAG staining and western blots, **(C)** by MBP staining and western blots, by **(D)** NF-H, NF-M, NF-L staining and western blots. No obvious axon injury detected by neurofilament-heavy (NF-H), neurofilament-medium (NF-M), neurofilament-light (NF-L) staining and western blots until three months post-BCAS. **(E)** Representative coronal sections illustrate the temporal progression of myelin injury detected by diffusion tensor imaging (DTI). (Interaural 4.90mm, Bregma 1.10mm for upper section and Interaural 2.10mm, Bregma -1.70mm for lower section in a-e; CCm: the medium part of corpus callosum; CCp: peripheral part of corpus callosum, AC: anterior commissure, F: fimbria of the hippocampus; IC: internal capsule, OT: optic tract; DTI: diffusion tensor imaging).

**Supplementary Figure 6**
**Astrocytic activation post-hypoperfusion injury was attenuated by Cx43 inhibition.**
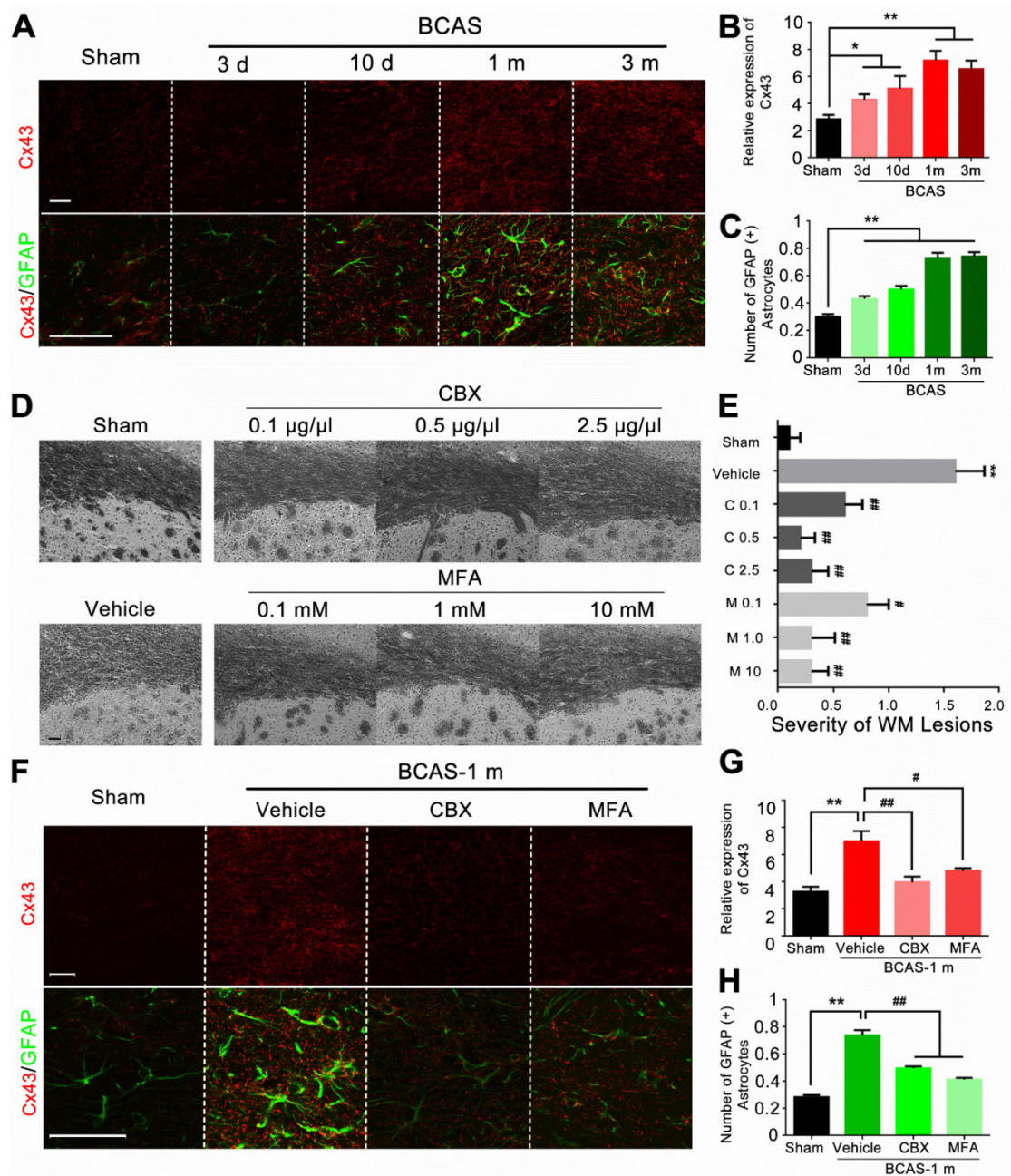


**(A)** Representative confocal images of coronal sections immunolabeled for Connexin43 (Cx43) and glial fibrillary acidic protein (GFAP) at three days, ten days, one month, and three months post-BCAS. Scale bar, 50µm. **(B-C)** Quantitative analysis of the expression of GFAP and Cx43 in **(A).** The unit for y-axis was $10^3/mm^2$. * p<0.05 ** p<0.01 versus Sham, one-way ANOVA with Dunnett's post-hoc test, n=6 mice per group. **(D)** The severity of white matter lesions was detected by luxol fast blue (LFB) staining in mice treated with series concentration of connexin43 inhibitors (0.1, 1, and 10 mM for meclofenamic acid (MFA) and 0.1, 0.5, and 2.5 µg/µl for carbenoxolone (CBX)). Scale bar, 50 µm. **(E)** Summary of the severity of white

matter lesions in **(D)** is shown as a histogram. ** $p<0.01$ versus Sham, # $p<0.05$ ## $p<0.01$ versus Vehicle, one-way ANOVA with Dunnett's post-hoc test, n=10 mice per group. **(F)** Representative confocal images of coronal sections labeled with Cx43 and GFAP in mice treated with connexin43 inhibitors (CBX, 0.5μg/μl and MFA, 1mM) at one month post-BCAS injury. Scale bar, 50 μm. **(G-H)** Quantitative analysis of GFAP and Cx43 expression in **(F)**. One-way ANOVA with Dunnett's post-hoc test, n=6 mice per group.

**Supplementary Figure 7**
**Long term intraventricular CBX, MFA, Gap19 and Gap26 infusion did not cause cognitive damage and white matter injury in control mice.**
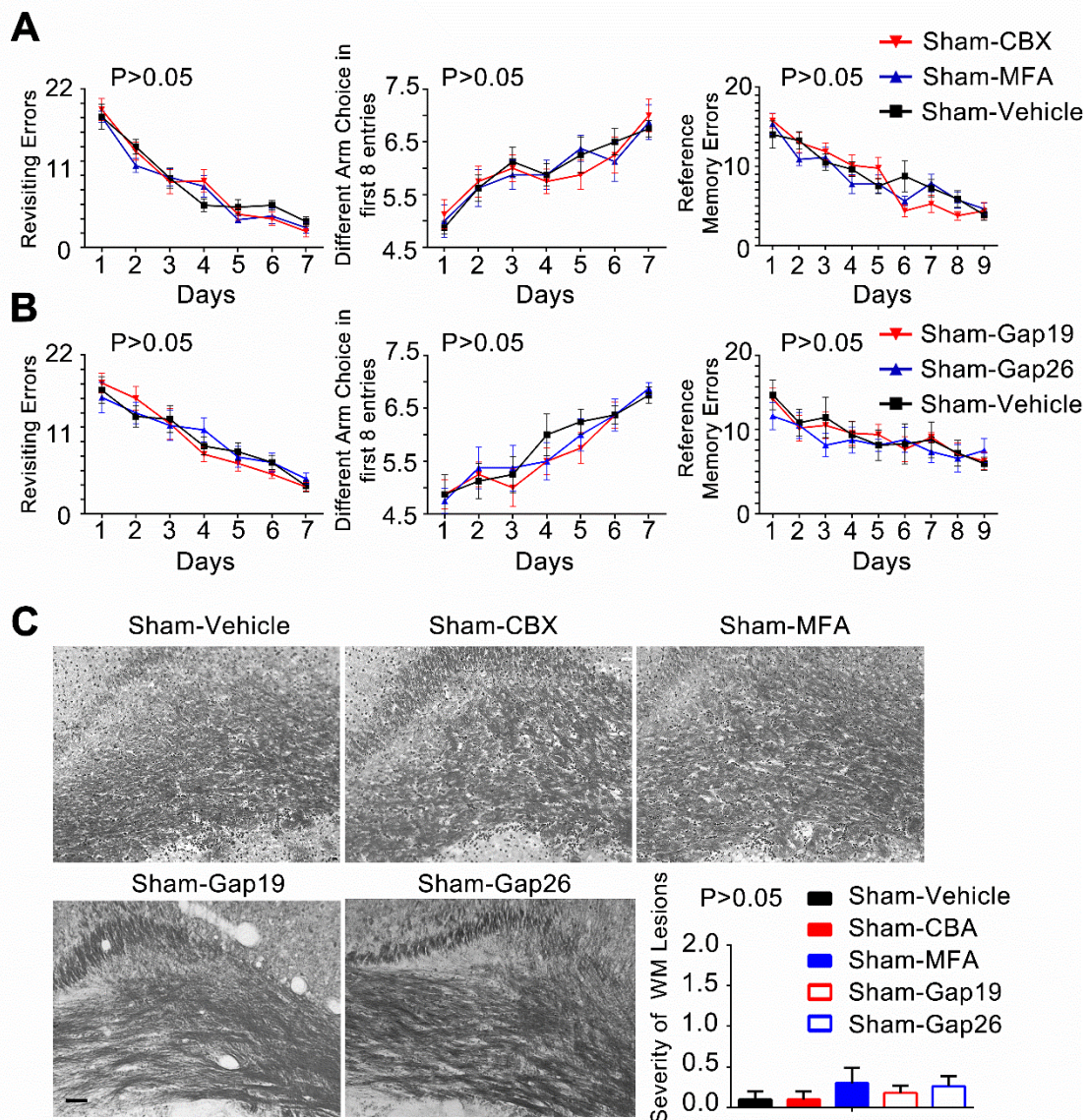


**(A)** The working memory of wild-type mice receiving continuous intraventricular infusion for one month with meclofenamic acid (MFA), carbenoxolone (CBX) or Vehicle was assessed by the eight-arm maze test. One-way ANOVA with repeated analysis, n=8 mice for each group. **(B)** The working memory of wild-type mice with infusion of Gap19, Gap26 or Vehicle was assessed by the eight-arm maze test. One-way ANOVA with repeated analysis, n=8 mice for each group. **(C)** Myelin loss was detected by luxol fast blue (LFB) staining in the medial part of the corpus callousm (CCm), striatum (CPu), anterior commissure (AC), internal capsule (IC), and fimbria of hippocampus (F) in wild-type mice with continuous intraventricular infusion with CBX, MFA, Gap19, Gap26, or Vehicle. Scale bar, 50 μm. The histogram summarizes the severity of white matter lesions. One-way ANOVA with Dunnett's post-hoc test, n=6 mice for each group.

**Supplementary Figure 8**
**Characterization of the astroglia-specific connexin43 conditional knockout mice.**
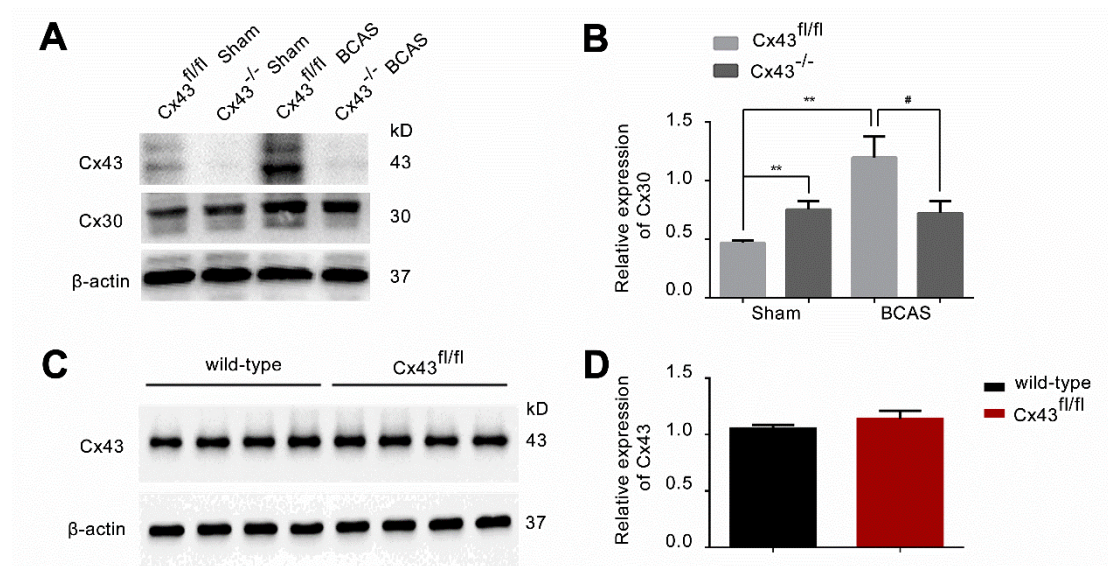


**(A)** The expression of connexin30 was detected in Cx43$^{fl/fl}$ mice and GFAP-Cre$^+$ Cx43$^{fl/fl}$ (Cx43$^{-/-}$) mice at one month post-BCAS as well as in sham-operated mice. **(B)** Quantitative analysis of **(A)**. **$p<0.01$ versus Cx43$^{fl/fl}$ Sham, #$p<0.05$ versus Cx43$^{fl/fl}$ BCAS, one-way ANOVA with Dunnett's post-hoc test, n=6 mice per group. **(c)** The expression of connexin43 detected in Cx43$^{fl/fl}$ mice and wild-type controls. **(D)** Quantitative analysis of **(C)**. $p>0.05$ versus wild-type controls, 2-tailed Student's t-test, n=6 mice per group.

**Supplementary Figure 9**
**Oligodendrocyte distress could be reduced by ablation of Cx43 post BCAS.**

**(A)** Representative confocal images of coronal sections immunolabeled for glutathione-s-transferase π (GSTπ) and 4', 6-diamidino-2-phenylindole (DAPI) in Cx43$^{fl/fl}$ mice and GFAP-Cre$^{+}$ Cx43$^{fl/fl}$ (Cx43$^{-/-}$) mice at one month post BCAS and in sham-operated controls. Scale bar, 50 μm. **(B)** Quantitative analysis of the GSTπ positive cell numbers in **(A)**. *p<0.05 **p<0.01 versus Sham, ##p<0.01 versus Cx43$^{fl/fl}$ BCAS mice, one-way ANOVA with Dunnett's post-hoc test, n=8 mice per group.

**Supplementary Figure 10**
**Axonal damage could be rescued by either pharmalogical blockade or genetic ablation of Cx43 post BCAS.**
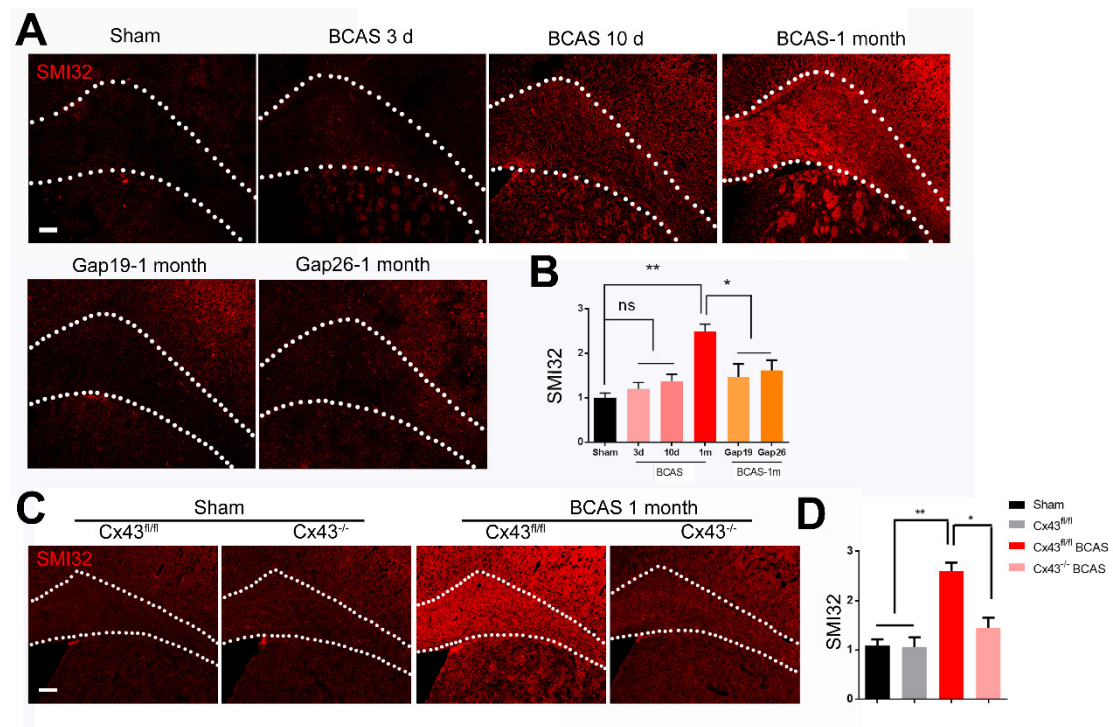


(A) Representative confocal images of coronal sections immunolabeled for the axonal marker SMI32 in mice at three days, ten days and one month post BCAS as well as their sham-operated controls and from mice treated either with Gap19 or Gap26 at one month post BCAS. Scale bar, 100 μm. (B) Quantitative analysis of the SMI32 fluorescence intensity in (A). (C) Representative confocal images of coronal sections immunolabeled for the axonal marker SMI32 in Cx43$^{fl/fl}$ mice and GFAP-Cre+ Cx43$^{fl/fl}$ (Cx43$^{-/-}$) mice at one month post-BCAS as well as in sham-operated mice. (D) Quantitative analysis of the SMI32 fluorescence intensity in (c) *p<0.05, **p<0.01 lesion versus sham, one-way ANOVA with Dunnett's post-hoc test, n=5 mice per group.

**Supplementary Figure 11**
**The effect of Cx43 deletion on white matter ischemic injury at three months post BCAS**
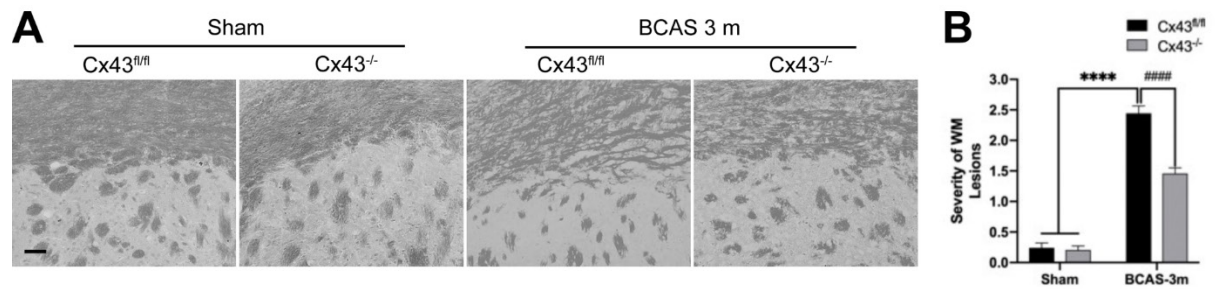


(A) Representative LFB staining of coronal sections in Cx43$^{fl/fl}$ mice and GFAP-Cre$^{+}$ Cx43$^{fl/fl}$ (Cx43$^{-/-}$) mice at three months post BCAS as well as their sham-operated controls. Scale bar, 50 µm. (B) Quantitative analysis of severity of WM lesions in (A). ****p<0.0001 lesion versus sham, ####p<0.0001 versus Cx43$^{fl/fl}$ BCAS mice, one-way ANOVA with Dunnett's post-hoc test, n=6 mice per group.

**Supplementary Figure 12**

**Disruption of axon-myelin integrity could also be rescued by administering the Cx43 mimetic peptides Gap19 or Gap26 for 3 days.**
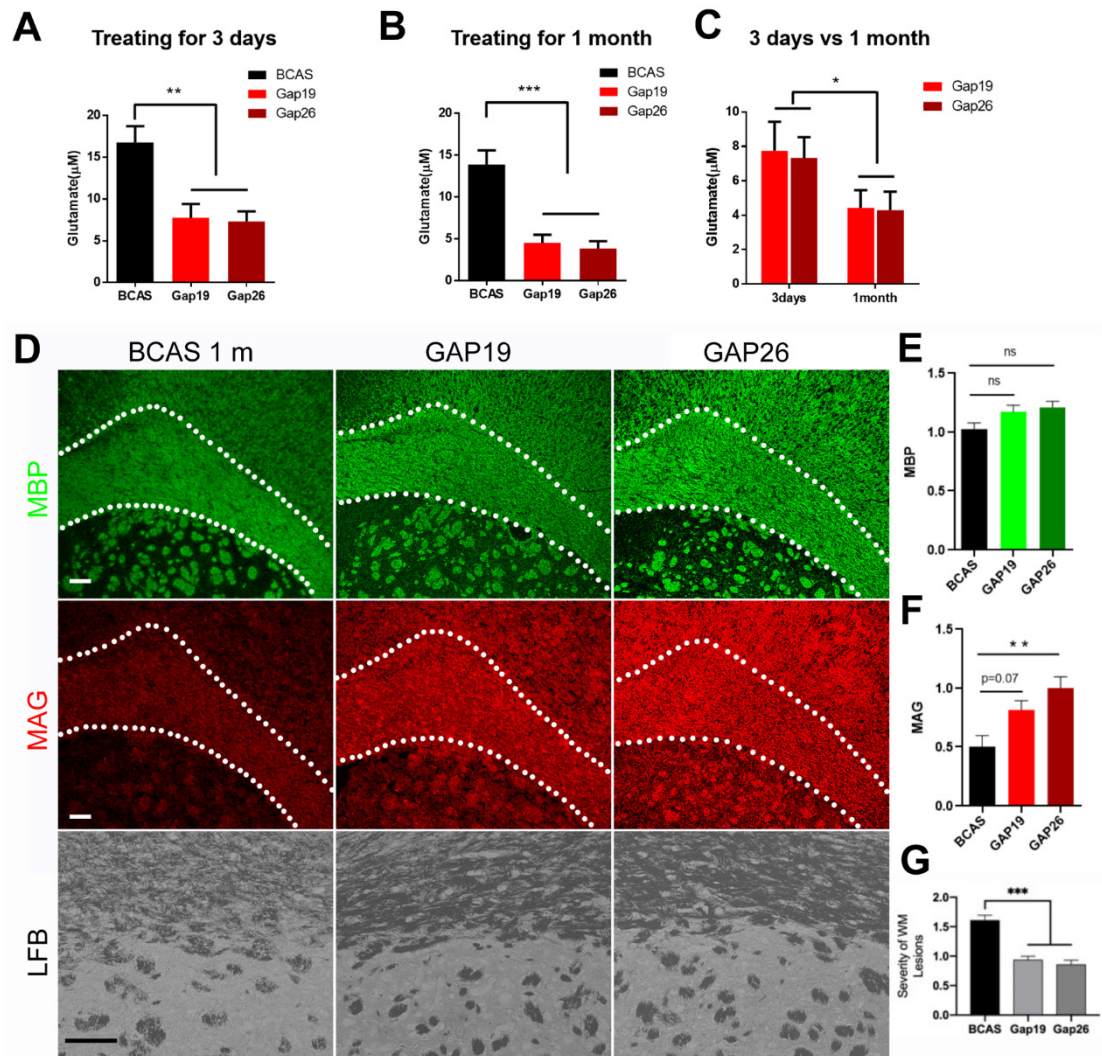


**(A, B)** The interstitial concentrations of glutamate in corpus callosum of n BCAS mice treated with Gap19 and Gap26 as well as vehicle controls for three days **(A)** and one month post-surgery **(B)**. **(C)** Comparison of the extracellular glutamate content in BCAS mice treated with Cx43 mimetics for three days and for one month. **(D)** Representative images of MBP, MAG immunolabeling and LFB staining in mice treated with vehicle, Gap19 or Gap26 for three days and one month post BCAS. Scale bar, 100 μm. **(E)** Quantitative analysis of the MBP fluorescence intensity in **(D)**. **(F)** Quantitative analysis of the MAG fluorescence intensity in **(D)**. **(G)** Quantitative analysis of severity of WM lesions in **(D)**. **p<0.01 ***p<0.001 sham versus BCAS, one-way ANOVA with Dunnett's post-hoc test, n=6 mice per group.

**Supplementary Figure 13**
**BCAS-associated microglial activation was retained by knockout of astroglial connexin43**
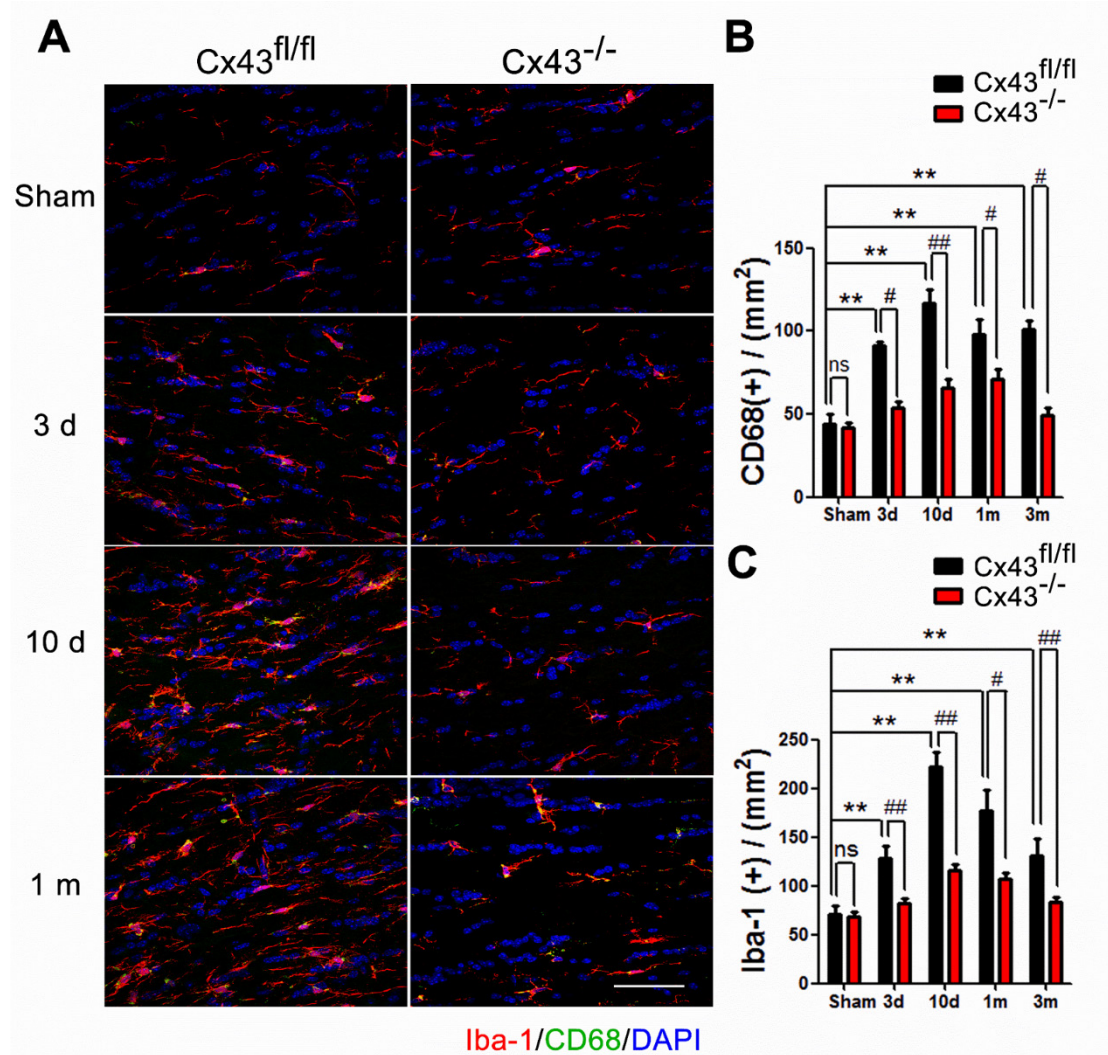


(A) Representative confocal microscopy images of coronal sections labeled with the microglial markers ionized calcium-binding adapter molecule 1 (Iba-1), Cluster of Differentiation 68 (CD68), and 4', 6-diamidino-2-phenylindole (DAPI) in Cx43$^{fl/fl}$ mice compared to GFAP-Cre$^+$ Cx43$^{fl/fl}$ (Cx43$^{-/-}$) mice at different time points (three days, ten days and one month) post-BCAS injury. Scale bar, 50 μm. **(B-C)** Quantitative analysis of the Iba-1 and CD68 positive cell numbers in **(A)**. ns, $p>0.05$, **$p<0.01$ versus Cx43$^{+/+}$ Sham, #$p<0.05$, ##$p<0.01$ versus Cx43$^{+/+}$ BCAS mice, one-way ANOVA with Dunnett's post-hoc test, n=6 mice for each group.

**Supplementary Figure 14**

**Decreased cytokine levels were observed in astrocytic Cx43 knockout mice post BCAS injury.**
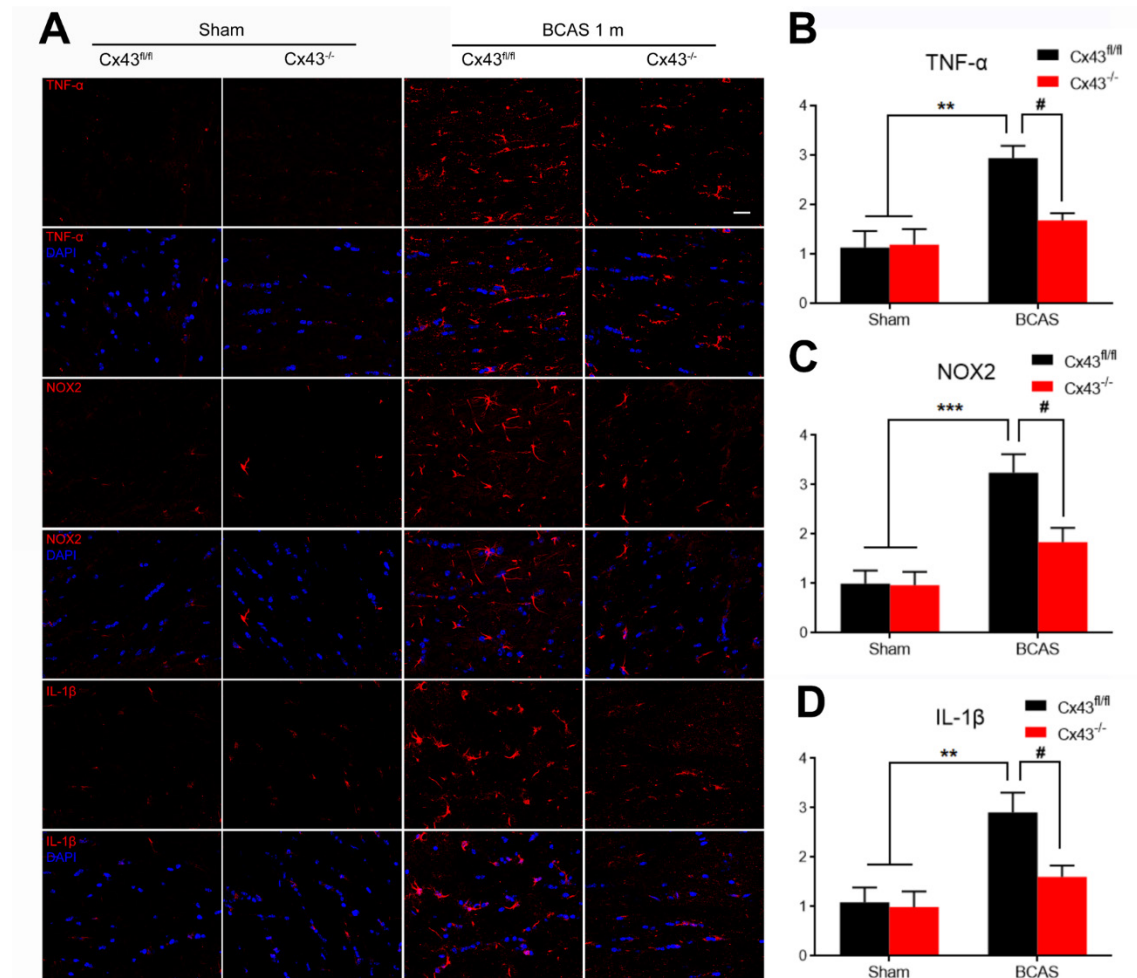


**(A)** Representative confocal images of coronal sections immunolabeled for TNF-α, NOX2 and IL-1β in Cx43$^{fl/fl}$ mice and GFAP-Cre+ Cx43$^{fl/fl}$ (Cx43-/-) mice at one month post BCAS as well as their sham-operated controls. Scale bar, 20 μm. **(B)** Quantitative analysis of the TNF-α positive cell numbers in **(A)**. **(C)** Quantitative analysis of the NOX2 positive cell numbers in **(A)**. **(D)** Quantitative analysis of the IL-1β positive cell numbers in **(A)**. **p<0.01 ***p<0.001 versus Sham, #p<0.05 versus Cx43$^{fl/fl}$ BCAS mice, one-way ANOVA with Dunnett's post-hoc test, n=6 mice per group.

## Supplemental References

1.    Theis M, de Wit C, Schlaeger TM, Eckardt D, Kruger O, Doring B, et al. Endothelium-specific replacement of the connexin43 coding region by a lacZ reporter gene. Genesis. 2001; 29: 1-13.

2.    Theis M, Jauch R, Zhuo L, Speidel D, Wallraff A, Doring B, et al. Accelerated hippocampal spreading depression and enhanced locomotory activity in mice with astrocyte-directed inactivation of connexin43.J Neurosci. 2003; 23: 766-76.

3.    Reimer MM, McQueen J, Searcy L, Scullion G, Zonta B, Desmazieres A, et al. Rapid disruption of axon-glial integrity in response to mild cerebral hypoperfusion. J Neurosci. 2011; 31: 18185-94.

4.    Tress O, Maglione M, May D, Pivneva T, Richter N, Seyfarth J, et al. Panglial gap junctional communication is essential for maintenance of myelin in the CNS. J Neurosci. 2012; 32: 7499-518.

5.    Shibata M, Yamasaki N, Miyakawa T, Kalaria RN, Fujita Y, Ohtani R, et al. Selective impairment of working memory in a mouse model of chronic cerebral hypoperfusion. Stroke. 2007; 38: 2826-32.